A new approach to railway track switch actuation

Dutta, Saikat; Harrison, Tim; Ward, Christopher Patrick; Dixon, Roger; Tara, Scott

DOI:
10.1177/0954409719868129

A new approach to railway track switch actuation: Dynamic simulation and control of a self-adjusting switch

Proc IMechE Part F: JRail and Rapid Transit
XX(X):1–9

DOI: 10.1177/ToBeAssigned
www.sagepub.com/

Saikat Dutta[1], Tim Harrison[2], Christopher Patrick Ward[2], Roger Dixon[1] and Tara Scott[3]

Abstract

The track switch is one of the key assets in any railway network. It is essential to allow trains to change route; however, when it fails significant delays are almost inevitable. A relatively common fault is 'loss of detection', which can happen when gradual track movement occurs and the switch machines (actuators) no longer close the gap between the switch rail and stock rail to within safe tolerances. Currently, such misalignment is mitigated by a preventative programme of inspection and manual re-adjustment. In contrast to many other industries, the actuators are exclusively operated in open-loop with sensors (often limit switches) mainly being used for detection. Hence, an opportunity exists to investigate closed-loop control concepts for improving the operation of the switch.

This paper proposes two advances; first, a novel approach is taken to modelling the dynamic performance of track switch actuators and the moving permanent-way components of the switch. The model is validated against real data from an operational switch. Secondly, the resulting dynamic model is then used to examine the implementation of closed-loop feedback control as an integral part of track-switch actuation. The proposed controller is found to provide suitable performance and to offer the potential of 'self-adjustment' i.e., re-adjust itself to close any gap (within a predefined range) between the stock and switch rails; thereby completing the switching operation.

Keywords

Railway track switch, Self-adjusting switch, Multibody simulation, Actuator, Closed loop control, Co-simulation

Introduction

Figure 1. High Performance Switch System (HPSS)

Railway switches are critical elements in a railway network. Any major failure in the switches can lead to derailment of the trains or to the vehicle taking an undesired path. The rails and the switches experience high amplitude dynamic loads from passing trains and the repeated nature of this load can cause misalignment in the switch layout. This is normally corrected manually during maintenance to prevent failure of the switch.

Bemment et al.[1] examined the failure rate of working switches in the UK railway network, documented by Network Rail between 1 April 2008 and 17 September 2011. Analysis was performed on the 39,339 fault/failure records that compared with the population of switches on UK mainline at 21,602. This data shows that the switches are very prone to failure. To prevent failure of the switch, the rules for switching operation are very conservative. A significant delay is caused if the switch fails in a dense-traffic route. Any misalignment in the switch layout is considered as a switch failure affecting the train service. The present work is a part of the project In2Rail[2] supported by the European Commission (EC) with a specific aim to develop a simulation model for a self-adjusting switch system.

There are a variety of railway switches which are in operation in the UK; among the most common are Clamplock, HPSS, HW and mechanical point machines.[3,4,5] Condition monitoring of switches is a topic in railway industry that has received much research attention. Its aim is to reduce and/or prevent any unexpected failure in the

[1] University of Birmingham, Birmingham, United Kingdom, B15 2TT
[2] Loughborough University, Leicestershire, United Kingdom, LE11 3TU
[3] Network Rail, Milton Keynes, United Kingdom, MK9 1EN

Corresponding author:
Saikat Dutta, , University of Birmingham, Birmingham, United Kingdom, B15 2TT.
Email: S.Dutta@bham.ac.uk

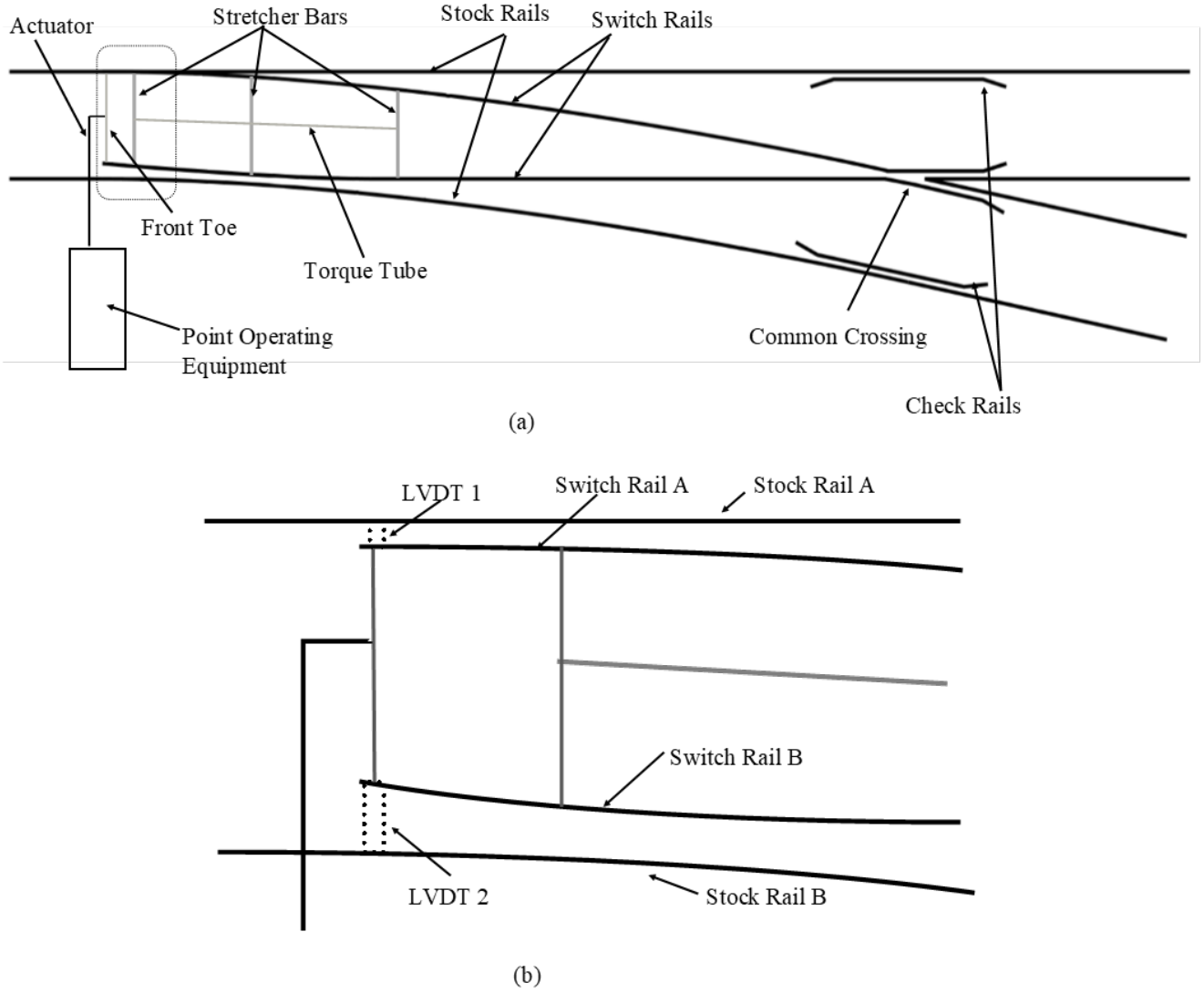

Figure 2. Schematic diagram of the HPSS track switch system: (a) full system; (b) Switch toe showing the LVDT positions during the switch travel

switches through condition based maintenance and studying the reliability of the switches.[6,7,8,9] Other researchers are tackling the problem by seeking to develop new actuation techniques or alternative switch layouts.[10,11]

Across the range of switch machines in the UK, closed-loop feedback control is not employed; nor has it been addressed in the literature. However, in principle it offers a range of benefits such as more accurate positioning, the ability to reject unwanted disturbances (such as misalignment), smoother dynamic trajectory and lower power.

There is also a gap in the literature (and practice) concerning high fidelity dynamic models of switch layout, actuators and the associated mechanisms. Such models are important for the design and study of closed-loop controllers. Hence, the objectives of the present paper are to develop a simulation model of a switch system, and develop a closed loop controller, then to design a self-adjusting algorithm to detect any misalignment (within a predefined range) in the switch or stock rail profile and re-align the switch rails to stock rails to close the gap so that the trains can pass safely over it. In this paper, the High Performance Switch System (HPSS) as used in UK rail network, is used as a case study (shown in Figure 1). First the switch layout and the configuration of the switch layout is explained. Then, the new model approach which exploits co-simulation between Simulink and Simpack is proposed. The resulting (open-loop) full switch model is validated against data obtained from an operational switch. After validating the model, a closed loop controller is developed using the gap feedback from the switch system. A self-adjusting algorithm is developed using the designed closed loop controller.

Configuration of the switch layout

A schematic diagram of the switching layout of HPSS is shown in Figure 2. The switch panel is a traditional switch layout where the switch rails are actuated at the toe by the lead-screw of the actuator. A set distance between the rails is maintained through three stretcher bars. Maintenance of the stretcher bars is of high importance as any failure to these may cause major accidents.[12] Apart from the opening in the toe of the switch, one of the functions in the switch layout is to provide a defined gap at the third

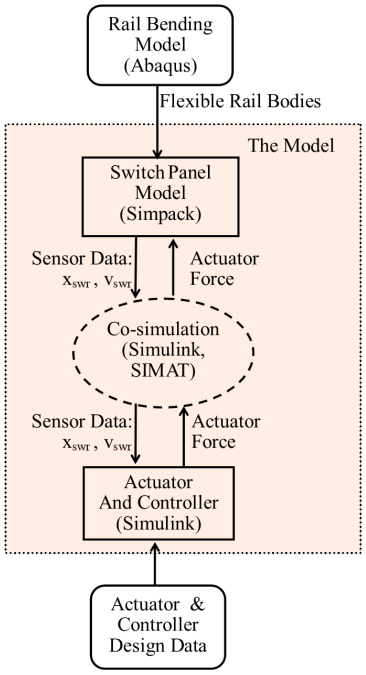

Figure 3. Modelling Approach

stretcher bar position. Conventional switches, sometimes use an additional backdrive to maintain the required gap at the backend of the layout. In the switch layout considered in this research, the front and rear stretcher bars are linked by a torque tube, which drives the rear end of the switch to ensure the desired gap. This switch configuration is equipped with Linear Variable Differential Transformers (LVDT) between the stock rails and switch rails at the toe position so that a measurements of the switch travel at the toe position can be used. Figure 2 shows the locations of the LVDTs.

The switch rails are locked at one position and upon command from the signalling block, the switch rails are unlocked. The actuator moves the front toe of the switch panel. The switch rails slide from one position to the other. The positions of the switch rail are detected and then locked. A non-backdrivable lead screw is used to lock the switch rails in its position and it is supported by an electronically actuated brake on the motor. In conventional switches, an additional mechanism is used, in some cases, to drive the rear part of the switch to ensure the desired profile of the switch rails.

Simulation model of full switch system

The full switch system consists of two major parts, namely, the switch panel and the actuator. The switch panel includes all the rail elements and the bodies connected to the rails. The actuator receives power from the lineside cabinet or the Point Operating Equipment (POE) and drives the front toe to move the switch rails from one position to the other. These elements are modelled in two different ways which are shown in Figure 3. The actuator bearer parts along with the newly designed controller are modelled in Simulink. A multi-body simulation model of the switch panel is developed in Simpack. The switching operation is dependent on bending of the rails. Thus, a finite element analysis of the rails is necessary to model the system. Hence, the rails are

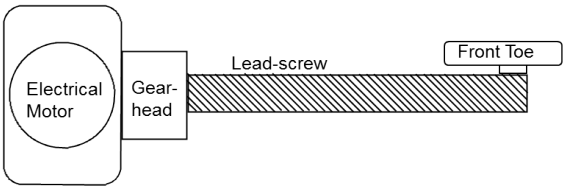

Figure 4. Schematic diagram of the actuator of the switch system

created as flexible bodies in Simpack using the finite element bodies created in Abaqus. A co-simulation between Simulink and Simpack can be obtained using SIMAT environment which is explained in the literature.[13,14] The inputs to the Simulink model are the sensor data i.e., displacement (x_{swr}) and velocity (v_{swr}) of the switch rails which are the outputs of the Simpack model. The input to the Simpack model is the actuator force which is the output of the Simulink model (shown in Figure 3). The data exchange between Simpack and Simulink models during the co-simulation is synchronised with fixed time steps in the SIMAT co-simulation environment without modifying the input and output signals. The co-simulation results are then validated against the data from a working switch system.

Actuator model in Simulink

The actuator is an electro-mechanical system consisting of electrical motor, gearbox and a lead-screw. The schematic representation is shown in Figure 4. The front toe of the switch panel is connected to the lead-screw through mechanical linkages.

The motor is connected to speed-reduction gearbox. The governing equations of the electrical motor are shown in equation 1.

$$V_M = I_A R_A + L_A \dot{I}_A + K_V \dot{\omega}_M \tag{1}$$

where,

V_M Motor voltage

I_A Motor current

R_A Armature resistance

L_A Armature inductance

K_V Back emf constant of the motor

ω_M Motor angular velocity

$$T_M = I_A K_T \tag{2}$$

where,

T_M Motor electrical torque

K_T Torque constant of the motor

The shaft connecting the motor output shaft and the gearhead input shaft is very small. Thus, the torsional effect of the shaft is neglected. The governing equation is given as

$$(J_M + J_g)\ddot{\theta}_M + (B_M + B_g)\dot{\theta}_M = T_M - \frac{T_{go}}{n_g} \tag{3}$$

where,

J_M Motor Inertia

J_g Gearhead Inertia

B_M Motor frictional coefficient

B_g Gearhead frictional coefficient

θ_M Motor angular position

T_{go} Gearhead output torque

n_g Gear Ratio

The load torque on the gearhead is generated from the rotational stiffness between the output shaft of the gearhead and the lead-screw.

$$T_{go} = K_{gh}\{\theta_{go} - 2\pi x_{ls}/l_s\} + C_{gh}\{\omega_{go} - 2\pi v_{ls}/l_s\} \quad (4)$$

where,

K_{gh} Rotational Stiffness of the gearhead

C_{gh} Rotational damping of the gearhead

θ_{go} Gearhead output angular position

x_{ls} Lead-screw linear displacement

l_s Lead of the screw

ω_{go} Angular velocity of gearhead output shaft

v_{ls} Lead-screw linear velocity

The lead-screw converts the rotating motion of the gearhead output shaft to linear motion at the front toe. Backlash between the lead-screw and the gear-head assembly is not considered in the modelling as this is negligible on this system. The rotational equation of motion is written by,

$$J_{ls}\ddot{\theta}_{ls} + B_{ls}\dot{\theta}_{ls} = T_{go} - T_L \quad (5)$$

where,

J_{ls} Lead-screw Inertia

θ_{ls} Lead-screw angular position

B_{ls} Lead-screw frictional coefficient

T_L Load Torque on the lead-screw

The linear velocity and the rotational velocity of the lead-screw are related as,

$$\begin{aligned} v_{ls} &= \omega_{ls} l_s/2\pi \\ x_{ls} &= \theta_{ls} l_s/2\pi \end{aligned} \quad (6)$$

The lead-screw is connected with the front-toe through a series of bars which is modelled as a stiff spring-damper assembly such that the linear motion of the lead-screw and the front-toe remains the same (i.e., it approximates a rigid connection). The force, which the actuator exerts on the front-toe, is calculated as

$$F_L = C_{fs}(v_{ls} - v_{ft}) + K_{fs}(x_{ls} - x_{ft}) \quad (7)$$

where,

F_L Load on the lead-screw

C_{fs} Damping of the Lead-screw and front-toe mechanical assembly

K_{fs} Stiffness of the lead-screw and front-toe mechanical assembly

v_{ft} Front-toe velocity

x_{ft} Front-toe displacement

The load torque on the lead-screw assembly is

$$T_L = F_L l_s/2\pi \quad (8)$$

The output from the actuator model is the force, which acts on the front-toe of the switch panel modelled in Simpack. The inputs to this actuator model in Simulink are the displacement and velocity at the toe of the switch panel.

Switch panel model in Simpack

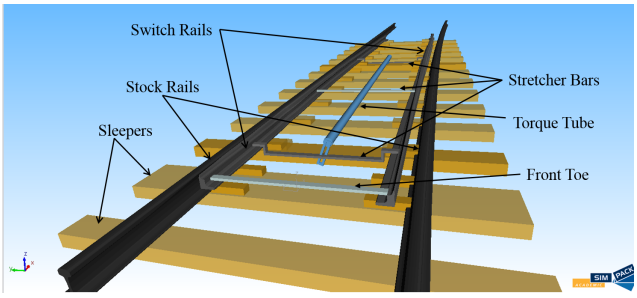

Figure 5. Switch panel model in Simpack

The switch layout for a CVS C-switch (vertical shallow depth)[3] is considered in this study. The rail elements are modelled using Finite Element (FE) analysis first in Abaqus and flexible bodies are generated through the FE analysis. The CAD model for switch rails and the stock rails are imported to Abaqus and converted into flexible (.fbi files) bodies for modelling in Simpack. The points of contact of the rail bodies with other bodies like the stock rails, stretcher bars, sleepers and front toe are generated as nodes during the FE analysis. The material of the rail bodies is modelled as isotropic steel and the FE mesh is constructed using second order quadratic tetrahedral elements.

Thereafter, the full switch panel model of the system is created using multibody simulation software Simpack (shown in Figure 5) with the flexible rail bodies and other rigid bodies. The different force elements like the friction forces between sleepers and the switch rails, the contact force between the switch rail and the stock rail are included in the Simpack model of the switch layout.

Co-simulation of the full system

The next part of the modelling is to form the co-simulation environment which combined the actuator with panel in order to simulate the complete switch system. The co-simulation between Simpack and Simulink is created using SIMAT interface in Simulink, which is shown in Figure 6. The actuator receives the displacement data from the Simpack model and the output is the actuation force to the

lead-screw. The input to the Simpack model is the actuator force and the output are the data from sensors in the Simpack model.

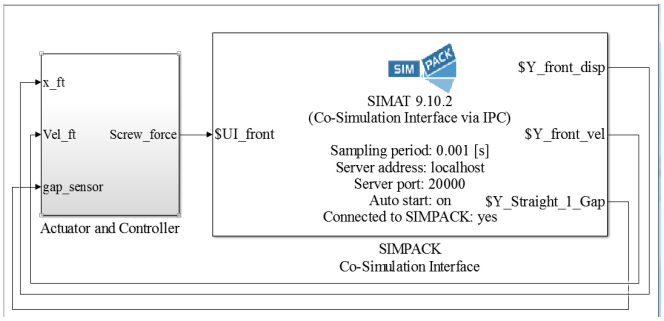

Figure 6. Co-simulation between Simpack and Simulink using SIMAT interface in Simulink

Model validation

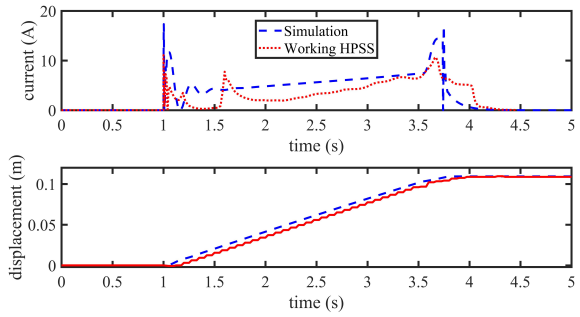

Figure 7. Model validation for the motor current and toe displacement

The model is validated against data supplied by Network Rail, UK for a real switch machine under test. The data available are the motor current and the displacement of the switch rails at toe position. In Figure 7, the simulation result is plotted against the working HPSS data. When the command is fed to the switch system to move (at time 1 s), the electrical motor is supplied with a constant voltage of 120V. As soon as the switch rail stalls against the corresponding stock rail to close the gap, the motor current rises and the motor is switched off. The simulation result shows a good agreement as the time (3.7 s) when the switch rail closes the gap matches with the experimental data and the rise in the current matches. The differences in the modelling data and test data are present due to difference in some parameters of the switch rail, such as the friction coefficient between the rails and sleeper, frictional coefficients, variable friction through the switch travel and other parameters, which are difficult to measure and simulate accurately.

Figure 7 also shows the displacement at the front toe, which shows that the front-toe displacement amplitude is 110 mm which matches the required switch rail travel. The next step of the study is to design a closed loop controller which is explained in the following section.

Controller design

This section presents a closed loop controller which will regulate the motion of the switch rails using feedback sensors placed to measure the gap from the existing system. The first step to design the controller is to define the control requirements. These are derived from the operating requirements of the switch system and discussion with industry colleagues. The technical specifications of the motor, are also given below.

Steady State Error: 0 mm - The difference between command and output in a steady state, i.e. unchanging situation.

Rise time: 3 s - Time taken to for the response to move from 10% to 90% of the command following a step change in command.

Settling time: 4 s - Time taken to become within 2% of the new steady state value following a step change.

Overshoot: 0% - The percentage of the overshoot beyond the steady state value.

Stability: Stability margins ensure the stability performance of the system in the presence of bounded model errors or changes in the system over time.

- Phase margin : $\geq 60°$
- Gain margin : ≥ 6 dB

Maximum voltage: 150 V - The maximum voltage of the motor is 190 V

Maximum current: 20 A - the maximum current to the motor is 24 A

A cascaded control system[15,16,17] is proposed to meet the control requirements. The designed controller consists of two cascaded control loops. The inner control loop acts on the current and the outer control loop performs the position control. The control layout is shown in Figure 8. The inner motor current control loop consists of a Proportional (P) controller and the outer position control loop includes a Proportional-Integral (PI) controller. The current loop is tuned first and then the position controller is tuned. The frequency responses are plotted using Control Design toolbox in Simulink, by linearizing and analysing the frequency response of the system. In the present configuration of the switch, two LVDT are connected with the front toe and the switch rails which is used for detection and locking with the consolidation of the two signals into one as shown in Figure 13 . The present research proposes individual LVDT to be connected to both the stock rails and their corresponding switch rails to measure the gap between the rails at the toe position, which is critical for a switch system. The sensor data from the LVDTs is then used as a feedback to the controller.

To design the controller, the actuator model is used and the bending force of the rails is considered as an external excitation in Simulink. Two different sets of controller parameters are designed for the current system depending on the duration of operation. For the switch layout considered in this study, the gap between the switch rail and stock rail at the

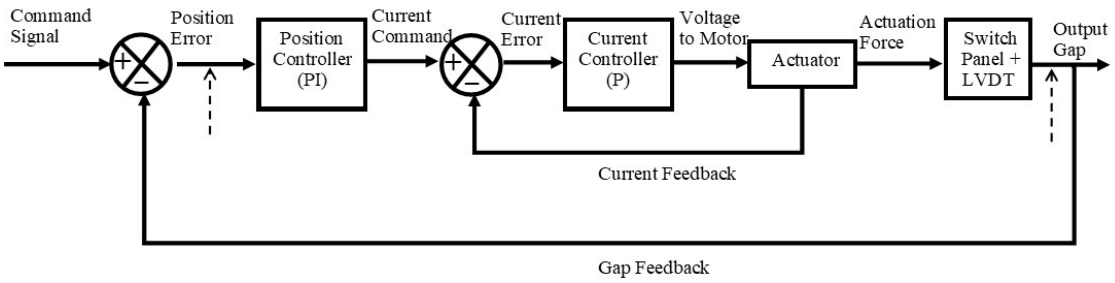

Figure 8. Controller layout for the switch system

open position is 110 mm. Upon receiving the command from signalling block, the gap command signal is set to zero to the controller (as shown in Figure 8). Both controllers satisfy the phase margin (PM) and gain margin (GM) requirements. The open loop frequency responses of the system with the designed controllers (shown as fast and slow) are plotted in Figure 9. The input and output measurement points of the system for obtaining the Nichols chart (Figure 9) are indicated by the dashed arrows on the block diagram of Figure 8. The chart shows the open-loop frequency response, gain vs phase, including the gain and phase margins.[18] The gain margins of the system, which are the distances between the critical point (0 dB, 180°) and the phase crossover point of the open-loop loci, are 61.4 dB and 70.6 dB for fast and slow controller respectively. The phase margins, which are the distances between the critical point and the gain crossover point, are 90° in both cases. The gain margin and phase margins for the selected controller parameters are well above the requirements, which ensures the stability of the closed-loop system. The controllers were not tuned to reduce the gain and phase margins because the requirements in the time domain were already satisfied.

The time response of the system are plotted in Figure 10 and the performance measures are tabulated in Table 1. The peak value of the voltage for the fast response (118.1 V) is much higher to that of the slow response (100.9 V) . The settling times for the fast and slow controller are 2.9 s and 3.6 s respectively, which are within the control requirement. The slow controller requires less power while satisfying all the control requirements. Thus, for further simulation task, the fast controller is selected. However, it is clear that faster performance is indeed possible if it were required.

Control Requirements	Unit	Fast	slow
Phase Margin	°	90	90
Gain Margin	dB	61.4	70.6
Rise Time	s	2.1	2.6
Settling Time	s	2.7	3.1
Peak Voltage	V	118.1	100.9
Peak Current	A	7.3	7.1
Peak Power	W	752.4	600.8

Table 1. Performance comparison of different closed loop controllers

The co-simulation is carried out with the designed fast controller. The sensor measures the gap between the switch rail and the stock rail and feedback to the controller unit (shown in Figure 8). The response of the system is plotted

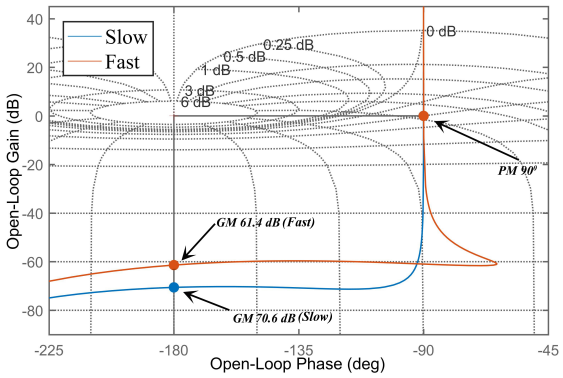

Figure 9. Nichols chart of the designed controller

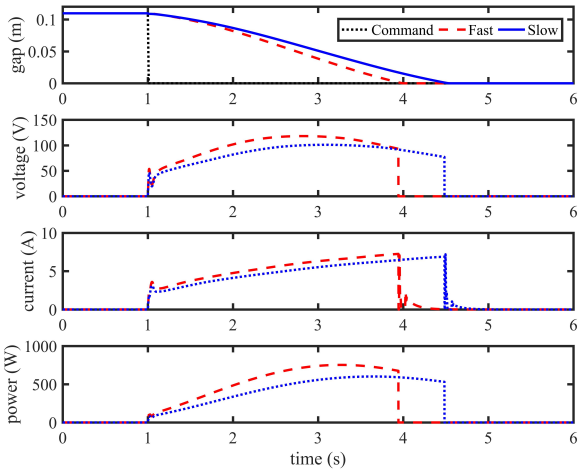

Figure 10. Comparison of performance of the system with two different controllers

against the open-loop response to compare the performance (Figure 11). The parameters are tabulated in Table 2. The RMS values are calculated over the period of 5 s (between 1 s and 6 s of Figure 11). It is seen that the closed loop system requires less power than the open loop system. The closed loop system is slower in terms of settling time by 0.1 s. But, the advantage of the closed loop system is that the motor does not run at a constant high 120 V voltage input, which reduces the power requirement during switching operation. The peak power during the switching is reduced by a considerable 63%. The settling time and the rise time of the closed loop

system are well within the control requirements as well as the peak voltage and current limits of the electrical motor.

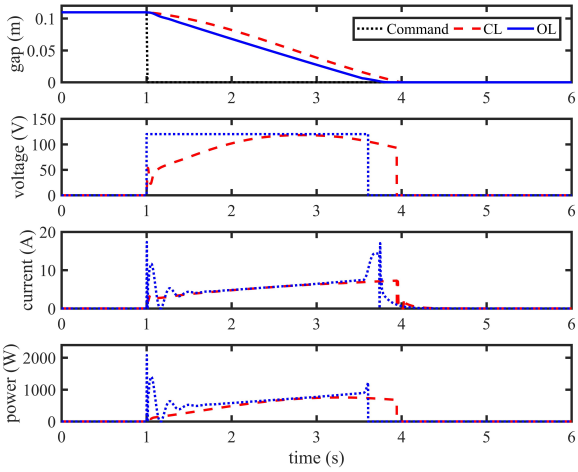

Figure 11. Comparison of performance of the open loop system and the system with the designed controller; OL: Open Loop, CL: Closed Loop.

Performance	Unit	OL	CL
Rise Time	s	2.1	2.1
Settling Time	s	2.6	2.7
Peak Voltage	V	120	118.1
Peak Current	A	17.2	7.3
Peak Power	W	2080.3	752.4
RMS Voltage	V	86.6	77.2
RMS Current	A	4.8	4.2
RMS Power	W	500.6	449.3

Table 2. Performance comparison of the closed loop (CL) system with the open loop (OL) system

Self-adjusting control strategy

A 'self-adjusting' switch should be able to detect any occurrence of misalignment (within a predefined range) between the stock rails and the switch rails or in the sleepers, and the controller should be able to re-align itself based on this information.

The misalignment was created in the switch panel modelling in Simpack. In the initial modelling, the stock rails were constrained so as to not to move in any direction and were fixed at the ideal set position. In the misaligned configuration, the stock rail was considered to displace a certain distance. In the Simpack model the stock rail at the toe position was allowed to be adjustable to a representation magnitude. The magnitude was set by a variable (x_{dis}) so that different displacements can be considered for the controller performance (shown in Figure 12). As the sensor is attached to the stock rail and the switch rail, it measures the relative position (gap) between the switch and stock rails and feeds the data back to the controller in Simulink.

The stock rails are displaced because of many reasons such as thermal expansion, environmental conditions, repeated dynamic load from running trains to name a few. The LVDT can be used to measure the gap between the stock rail and adjacent switch rail. The self-adjusting/inspecting switch rail feeds this gap sensor data back to the controller (shown in Figure 13). The self-adjusting algorithm first checks the gap. If the gap is within the allowable range (110 $\pm$ 10 mm), the desired gap command is passed to the actuator control system.

If the gap is beyond the range, it sends the fault signal to the signalling block. The time taken for sensing the gap and setting the new desired gap is 0.1 s in simulation. The new desired gap is set in the lock and detection algorithm. The controller works until the switch rail reaches the new position which is set by the self-inspecting algorithm and then it is locked and detected.

In the original open loop system, in presence of misalignment, if the switch rail travels more than its designed range, the LVDTs do not detect the switch rail positions and the actuator is stopped returning a fault signal. Thus, the open loop system does not close the gap in case of misalignment. In the proposed configuration, the self-adjusting algorithm will allow the switch rails to close the gap as the signal is fed back to the controller and the locking arrangement.

The performance of the self-adjusting algorithm as stated in Figure 13 is tested for different misalignment (x_{dis}) values. The value of misalignment (x_{dis}) is considered within $\pm$10 mm of the aligned layout. The co-simulation is carried out for three different misalignment magnitudes. The controller first senses the gap between stock rail and switch rails and checks the value to be in the predefined range. If the gap is within the range, the command gap signal is set to zero and the controller moves the rail. At the end of the controlled motion of the switch rail, the position of the switch rail is detected and signal is fed to the signalling block. The performance of the controller is shown in Figure 14. Three different displacements in the stock rail position are considered and the performance of the designed controller is tabulated in Table 3. It is seen that the self-adjusting logic is able to close the gap between the switch rail and the stock rail if the misalignment is within $\pm$ 10 mm range and the controller satisfies all the control requirements. It is also shown that the performance of the switch is maintained as the proposed controller is able to complete the switching task within the same time without human intervention.

Performance	Unit	x_{dis}		
		-10 mm	+5 mm	+10 mm
Rise Time	s	2.0	2.1	2.1
Settling Time	s	3.0	3.0	3.0
Peak Voltage	V	107.1	123.5	128.9
Peak Current	A	6.6	7.6	7.9
Peak Power	W	343.4	445.4	482.2
RMS Voltage	V	70.1	80.7	84.2
RMS Current	A	3.9	4.4	4.6
RMS Power	W	376.6	487.9	528.3

Table 3. Performance comparison of the self-adjusting control logic

Conclusions

This paper has presented a simulation model of a railway track switch and proposed a closed loop controller to obtain a self-adjusting switch system. The two major contributions of the present paper in the railway research are in modelling approach and introduction of closed loop controller in track

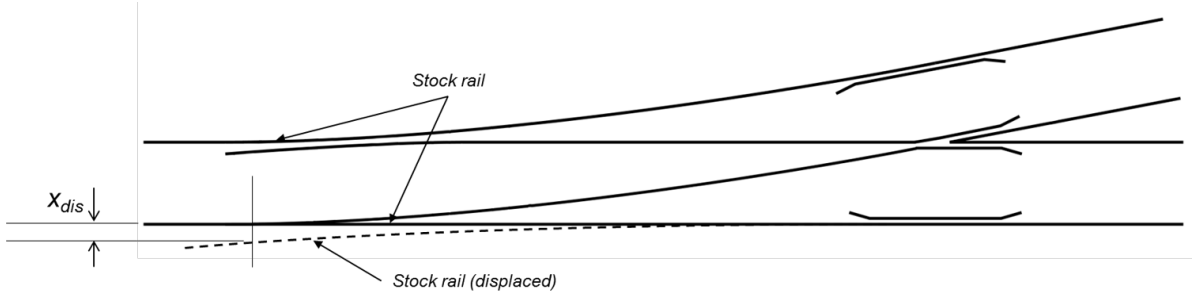

Figure 12. Schematic of the misalignment in the switch panel

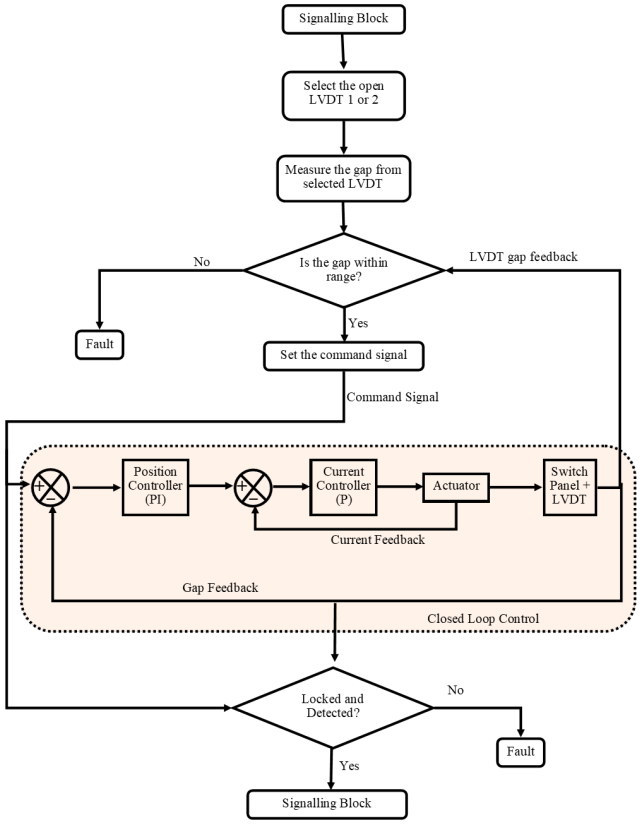

Figure 13. Algorithm for self-adjusting controller

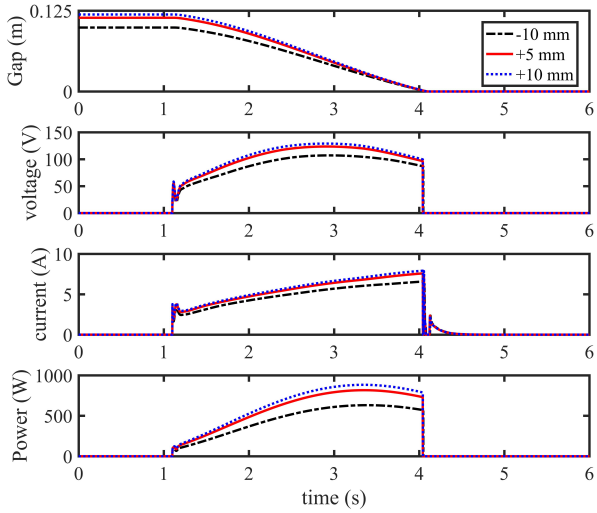

Figure 14. The performance of the self-adjusting controller for different amplitude of misalignment in the switch panel

switch operation. Firstly, the modelling approach, which is used to model an electro-mechanical switch system includes the flexible rail bodies, which model proper bending of the rails. The present model is validated against the working data from HPSS. Whilst this system is a very small percentage of the switch population of the European network, the overall modelling approach is generic and therefore can be used to model and simulate any other switch system (including hydraulic, pneumatic, electro-hydraulic). The outer control loop has to be modified for different kinds of POE. The other POEs will need different sensors to be integrated with the controller keeping the modelling approach unaltered. Secondly, a closed loop controller to control the switch movement is employed in the system which is not used in switching operation before. The designed controller is shown to perform the switching task while the power requirement is lower than the open loop operation. The introduction of self-adjusting algorithm along with the closed loop controller is shown to re-adjust a misalignment (within a predefined range). This has the potential to reduce the amount of manual maintenance required for switch misalignment and adjustment. This self-adjusting algorithm could decrease the amount of cyclical maintenance carried out on the unit, especially the Facing Point Lock test. Further research on safety and cost benefit analysis with failure data from existing S&C is needed to quantify the benefit. The next phase is to introduce a hardware in the loop (HIL) testing, which can be implemented to check the designed controller.

Acknowledgements

This research was supported by the European Unions ‘Horizon 2020 the Framework Programme for Research and Innovation (2014-2020)’ through grant number ‘635900’ for the project ‘IN2RAIL: Innovative Intelligent Rail’. The authors also gratefully acknowledge Network Rail for providing the drawings and data from the working HPSS.

References

[1] Bemment SD, Goodall RM, Dixon R, Ward CP. Improving the reliability and availability of railway track switching by analysing historical failure data and introducing functionally redundant subsystems. Proceedings of the Institution of Mechanical Engineers, Part F: Journal of Rail and Rapid Transit. 2017;232(5):1407–1424.

[2] In2Rail. In2Rail; 2018. Accessed: 2018-06-01. http://www.in2rail.eu/.

[3] Cope GH. British Railway Track: Design, Construction and Maintenance. Permanent Way Institution, UK; 1993.

[4] Morgan J. British Railway Track 7th Edition, Volume 1, Design Part 2: Switches and Crossings. Derby, UK: The Permanent Way Institution. 2009;.

[5] Lagos RF, Alonso A, Vinolas J, Pérez X. Rail vehicle passing through a turnout: analysis of different turnout designs and wheel profiles. Proceedings of the Institution of Mechanical Engineers, Part F: Journal of Rail and Rapid Transit. 2012;226(6):587–602.

[6] Rama D, Andrews JD. A reliability analysis of railway switches. Proceedings of the Institution of Mechanical Engineers, Part F: Journal of Rail and Rapid Transit. 2013;227(4):344–363.

[7] Marquez FPG, Weston P, Roberts C. Failure analysis and diagnostics for railway trackside equipment. Engineering Failure Analysis. 2007;14(8):1411–1426.

[8] Molina LF, Resendiz E, Edwards JR, Hart JM, Barkan CP, Ahuja N. Condition monitoring of railway turnouts and other track components using machine vision; 2011.

[9] Oyebande B, Renfrew A. Condition monitoring of railway electric point machines. IEE Proceedings-Electric Power Applications. 2002;149(6):465–473.

[10] Sarmiento-Carnevali M, Harrison TJ, Dutta S, Bemment SD, Ward CP, Dixon R. Design, construction, deployment and testing of a full-scale Repoint Light track switch (I). The Stephenson Conference: Research for Railways, Institution of Mechanical Engineeers (IMechE); 2017. p. 409–416.

[11] Wright N, Bemment S, Ward C, Dixon R. A model of a repoint track switch for control. In: Control (CONTROL), 2014 UKACC International Conference on. IEEE; 2014. p. 549–554.

[12] Branch RAI. Rail accident report: Derailment at Grayrigg 23 February 2007. Report. 2011;.

[13] Bei SY, Zhao JB, Zhang LC, Liu SH. Fuzzy Control and Co-Simulation of Automobile Semi-Active Suspension System Based on SIMPACK and MATLAB. In: Applied Mechanics and Materials. vol. 39. Trans Tech Publ; 2011. p. 50–54.

[14] Kozek M, Benatzky C, Schirrer A, Stribersky A. Vibration damping of a flexible car body structure using piezo-stack actuators. Control Engineering Practice. 2011;19(3):298–310.

[15] Lee Y, Park S, Lee M. PID controller tuning to obtain desired closed loop responses for cascade control systems. Industrial & Engineering Chemistry Research. 1998;37(5):1859–1865.

[16] Saleem A, Taha B, Tutunji T, Al-Qaisia A. Identification and cascade control of servo-pneumatic system using Particle Swarm Optimization. Simulation Modelling Practice and Theory. 2015;52:164–179.

[17] Dash P, Saikia LC, Sinha N. Automatic generation control of multi area thermal system using Bat algorithm optimized PD-PID cascade controller. International Journal of Electrical Power and Energy Systems. 2015;.

[18] Kuo BC. Automatic control systems. Prentice Hall PTR; 1987.